

# Alternative Approach Toward the Aging of Asphalt Binder

Bernhard Hofko, Florian Handle, Lukas Eberhardsteiner, Markus Hospodka, Ronald Blab, Josef Füssl, and Hinrich Grothe

Awareness that natural, financial, and energy resources are scarce goods has increased. Thus demand is growing for infrastructure that is not only of high quality but also efficient. Efficiency, in this case, aims to optimize cost and energy consumption over the complete life cycle of a structure. The objective is to build long-lasting infrastructure with low maintenance demands and with high recycling potential after it has reached the end of its service life. For bituminous bound materials, the aging of asphalt binder has a crucial impact on durability and recyclability. Because asphalt binder is organic by nature, the thermal and oxidative aging processes affected by chemical and structural changes occur when asphalt mixes first are produced and applied and continue over the course of their service life. Increasing stiffness and brittleness of the binder make pavement more prone to thermal and fatigue cracking. The interdisciplinary research project reported here worked toward a better understanding of the physicochemical fundamentals of asphalt binder aging, as well as of the impact of binder aging on the mechanical properties of asphalt binder and asphalt mixes. Through extensive chemical and mechanical analyses, a new model was developed to explain the aging process comprehensively (i.e., on the physicochemical and mechanical levels). Aging can be determined mathematically by micromechanical modeling. With the model presented in this paper, changes in asphalt binder as a result of aging (i.e., increasing brittleness and stiffness) can be explained.

Today the efficiency of road infrastructure includes optimized structural performance not only in terms of resistance to fatigue, rutting, and low-temperature cracking but also in terms of cost and energy consumption. Long-lasting pavement structures should minimize their cost and energy consumption throughout their service life. High recyclability is another objective to ensure so that high-value asphalt mix layers can be reused in new pavements after the end of their service life. These considerations are reflected in the legal framework of the European Waste Framework Directive (2008/98/EG), which follows a waste management hierarchy: prevent, recycle, recover, and dispose.

Asphalt binder has an essential impact on the increasing susceptibility to cracking of asphalt mix layers. Increasing brittleness and stiffness make flexible pavements more prone to low-temperature

and fatigue-induced cracking, which decreases the pavement life span significantly. Aging-resistant binders promote higher durability and thus pavements that are cost and energy efficient. In contrast, aging asphalt binder and related changes in its characteristics limit the recyclability of asphalt mixes (1, 2).

## OBJECTIVES

Binder aging plays an important role in the improvement of cost and energy efficiency in road pavements. Thus, within the ongoing research project Oekophalt Physicochemical Fundamentals on Asphalt Binder Aging for Efficient Recycling of Asphalt Mixtures, an interdisciplinary team works toward the following objectives:

- Understanding the underlying reasons and processes of asphalt binder aging on a physicochemical and mechanical level (3–10),
- Understanding the impact of asphalt binder aging on the mechanical behavior of asphalt mixes,
- Expanding the assessment of aging resistance of binders, and
- Developing improved laboratory aging methods for asphalt mix testing to reflect field aging more accurately.

This project was designed to bridge the gap between fundamental and applied sciences. A joint taskforce of researchers from applied material science, material chemistry, and mechanical modeling was formed to take up these objectives.

The interdisciplinary nature of the cooperating researchers enabled the formulation of a new, holistic understanding of asphalt binder aging, on the basis of the conjuncture of the three fundamentally different perspectives of physicochemical analysis, micromechanical modeling, and mechanical material characterization. Comprehensive analysis was carried out of asphalt binder and asphalt mix aging in the field and in the lab. Specimens were obtained from a number of test sites on the public road network, which were chosen to reflect a range of aging (between 3 and 24 years) and in different states of performance. In addition, a test field was constructed in September 2012 to monitor field aging of unmodified and styrene-butadiene-styrene-modified binder and asphalt mixes in close detail (11).

This paper focuses on one outcome of the project: a microphysical and micromechanical model of asphalt binder to describe aging and its effects on the mechanical behavior of asphalt binder.

## POTENTIALS AND SOURCES

To determine cause and effect with respect to asphalt binder aging has been the starting point for numerous research studies, such as Petersen et al. (12). This issue was included in the present project

---

B. Hofko, L. Eberhardsteiner, M. Hospodka, and R. Blab, Institute of Transportation, Research Center of Road Engineering, Vienna University of Technology, Gusshausstrasse 28/E230-3, 1040 Vienna, Austria, F. Handle and H. Grothe, Institute of Materials Chemistry, Vienna University of Technology, Getreidemarkt 9, 1060 Vienna, Austria, J. Füssl, Institute for Mechanics of Materials and Structures, Vienna University of Technology, Karlsplatz 13, 1040 Vienna, Austria. Corresponding author: B. Hofko, bernhard.hofko@tuwien.ac.at.

*Transportation Research Record: Journal of the Transportation Research Board*, No. 2505, Transportation Research Board, Washington, D.C., 2015, pp. 24–31. DOI: 10.3141/2505-04

to close some gaps and illustrate the physicochemical fundamentals related to asphalt binder aging. It is important to understand the potential factors and vulnerabilities of asphalt binder with respect to its aging. Because asphalt binder has been shown conclusively to be an inhomogeneous material, the microstructure of the material must be considered one of those potential factors.

A detailed fractionation was carried out of various asphalt binder samples according to their polarity. The basic standard for fractionation is ASTM D4124. Contrary to the standard, however, samples were separated into more fractions, as shown in Figure 1. More than 20 fractions were analyzed through various spectroscopic and microscopic means. The results were the basis for a revised model of the microstructure and thus binder aging, presented later in this paper.

Short-term aging of asphalt binder is well documented and described in the literature. Short-term aging occurs during mixing and compaction of asphalt pavements and within the next several hours thereafter, while the material is cooling down and expressing its microstructure. It is possible to distinguish two basic effects of the harsh manufacturing conditions: (a) thermal aging characterized by thermal decomposition of metastable molecules and evaporation of volatile components and (b) oxidative aging by oxidation of susceptible molecules (12). Both are promoted by the elevated temperatures and the high specific surface during mixing and laying. In addition, synergetic effects of both processes have to be considered, because molecules fragmented by oxidation may well be prone to evaporation. Long-term aging (LTA), however, occurs while the pavement layer is in service under climate and traffic loading and is far less understood. Although studies exist that address LTA, research is fragmented, and much scientific discussion on the subject continues.

Consideration of atmospheric chemistry to isolate reactants available in the field serves as a natural starting point when external

factors are determined that could have an impact on LTA (14). Studies usually state that atmospheric oxygen and ultraviolet radiation are the main sources of aging. Aging as a result of exposure to ultraviolet radiation does occur but is limited to the upper few micrometers of the binder. Atmospheric oxygen is not the only available oxidant. Possibly, it is only partially responsible for field aging. Other reactive gases, such as nitric oxides and especially ozone, are available as well, because exhaust gases promote their formulation. Concentrations of these gases (some ppbs) clearly are below the level of atmospheric oxygen, but the oxidation potential is significantly higher than the potential for relatively inactive oxygen, at least at temperatures that occur in the field [ $< +65^{\circ}\text{C}$  ( $150^{\circ}\text{F}$ )]. The oxidizing gases mentioned can explain aging in upper layers close to the surface. Water soluble oxidants (e.g.,  $\text{HNO}_3$ ,  $\text{H}_2\text{SO}_4$ ,  $\text{H}_2\text{O}_2$ ) can penetrate even deeper into a pavement structure. Again, the concentration may be low but, once the substances have penetrated the structure, they may stay there for a considerable time and thus promote aging far more severe than their direct impact might imply. An overview of proposed aging sources and their significance for different pavement layers is provided in Figure 2.

### MICROPHYSICAL MODEL

Different ideas exist on the structural composition of asphalt binder. A widely accepted idea is the micelle model (15). The basic idea of this model is that asphalt binder is a dispersion of nonsoluble or low-soluble molecules (micelles) within a matrix phase. However, the model is not to be confused with the classical micelle method, which assumes the existence of high weight asphaltenes, consecutively proved to be wrong (16). Different studies, which provided arguments for the micelle model and the fractionation analysis

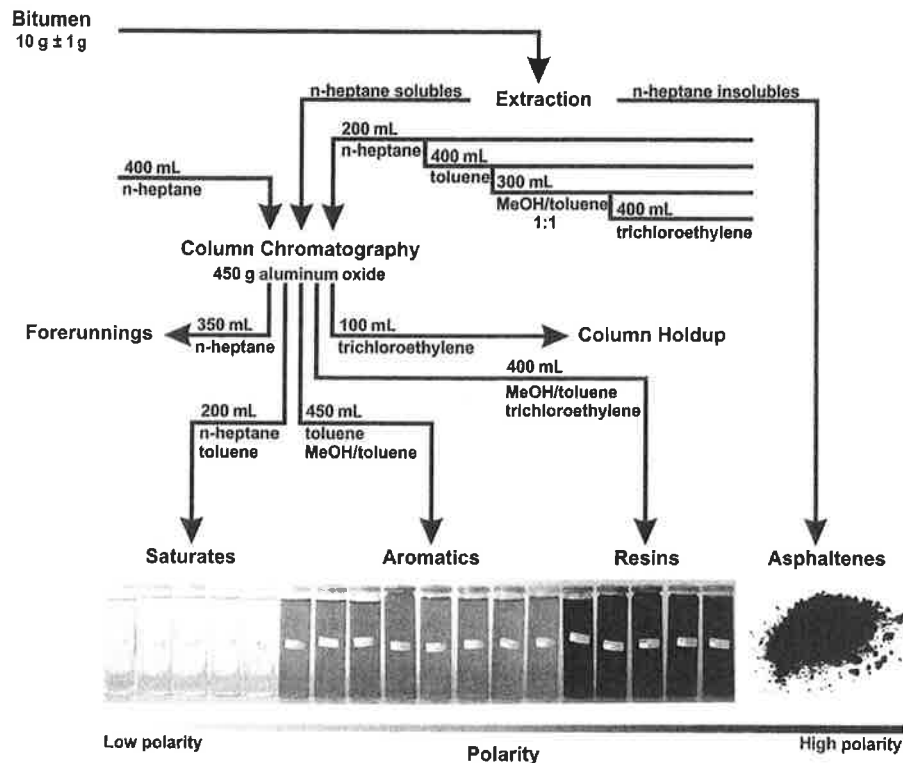


FIGURE 1 Binder fractionation in terms of polarity (13).

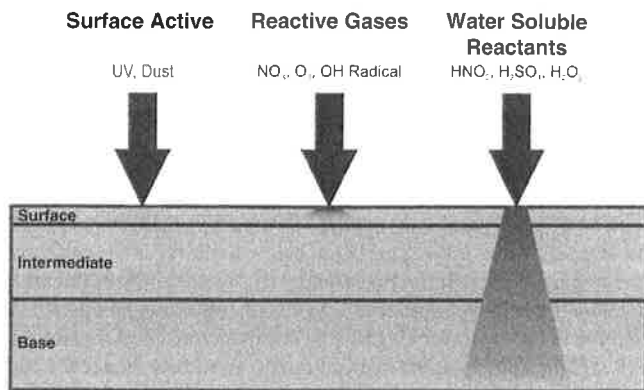
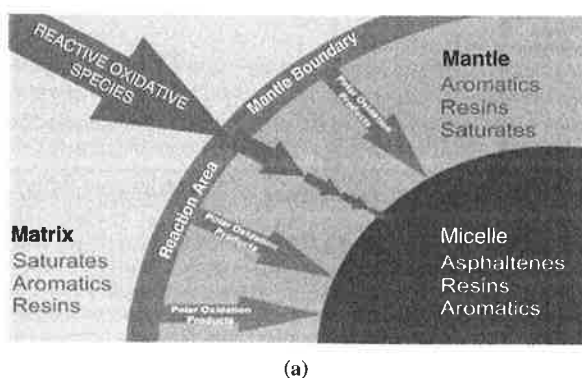
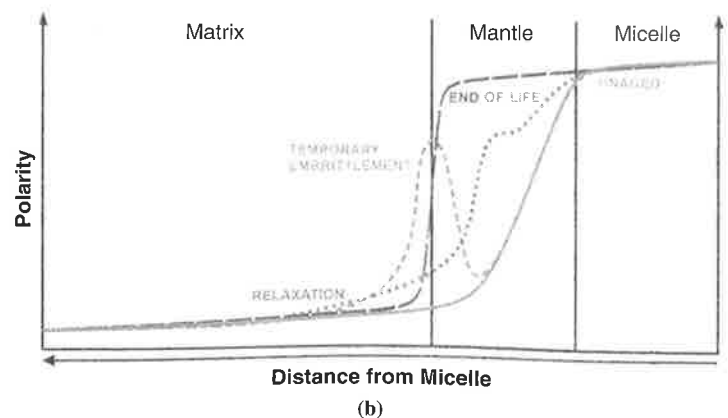


FIGURE 2 Available oxidants for aging of asphalt binder and asphalt mixes (13).

provided further evidence that highly polar asphaltenes were dispersed within a lowly polar matrix (maltene phase) of aromatics and saturates (17–23). To create a working dispersion, the highly polar asphaltenes need to be surrounded by a shell with a continuous polarity gradient to avoid phase separation processes. This state is shown in Figure 3b as the solid line for the unaged asphalt binder. Whereas the lowly polar maltene phase is inactive in terms of oxidation, the oxidation potential increases with increasing polarity. Because the highly polar asphaltene core is surrounded by a shell, the reactive oxidant species interact with the shell primarily, which leads to the formation of a reaction area rich in polar constituents. This effect can be healed by self-association processes, which lead to the diffusion of high-polar material into the micelle core, isolate it from the apolar matrix, and lead to the reformation of an intact, if slightly reduced, shell. With increasing aging, the process of oxidation leads to the disintegration of the shell, and eventually reaches the core after all. This state is shown in Figure 3b as the dotted line. Given the increasing oxidation of the shell, its polarity increases as well. This development leads to a loss of compatibility between micelles and the matrix as a result of the rising gap in polarity. This gap in polarity can be seen as a predetermined breaking point at the interface of shell and matrix. Macroscopic and mechanical testing correlates these effects to brittleness with progressing aging processes.



(a)



(b)

FIGURE 3 Reactive oxidant species interaction with (a) asphalt binder and (b) microphysical model of binder aging.

## MICROMECHANICAL MODEL

On the basis of the physicochemical analysis of asphalt binder and the microphysical model presented in the previous section, another objective of the research was to establish a micromechanical model of asphalt binder to analyze the impact of the microstructure on the macroscopic mechanical behavior of asphalt binder and impacts of aging on microstructure and mechanical behavior. For this purpose, the following steps were taken:

- An unmodified binder PG 58-22 was fractionated according to ASTM D4121-01 into the maltene and asphaltene phase. Precipitated blends of maltenes and asphaltenes with different well-defined asphaltene concentrations were produced.
- Atomic force microscopy (AFM) was carried out on the virgin binder, the maltene phase, and the precipitated blend with the same asphaltene concentration as the virgin binder to verify that the microstructure was reestablished after maltenes and asphaltenes were blended.
- Creep recovery (CR) tests were carried out at different temperatures on the virgin binder and the precipitated blends to study the impact of maltene and asphaltene on the overall mechanical behavior.
- A micromechanical model was established according to results of physicochemical and mechanical analyses of the samples.
- The same binder was aged with the use of a rolling thin-film oven test (RTFOT) and a pressure aging vessel (PAV) procedure to simulate long-term aging. The aged samples were again fractionated into the maltene and asphaltene phase, and precipitated blends were produced. CR tests were run and analyzed to study the impact of aging on microstructure and mechanical behavior.

To study the impact of both major fractions of asphalt binder, the maltene phase and the asphaltenes on the mechanical behavior, an unmodified binder PG 58-22 with an asphaltene concentration of 7.79 vol% according to ASTM D4121-01 was separated into the n-heptane soluble maltene phase and the n-heptane nonsoluble asphaltene phase on the basis of the procedure proposed by ASTM D4121-01. After extraction, n-heptane was evaporated from the maltene phase, and the asphaltenes and maltenes were dissolved in toluene and blended to samples with different well-defined asphaltene concentrations in the blend. Through evaporation of the

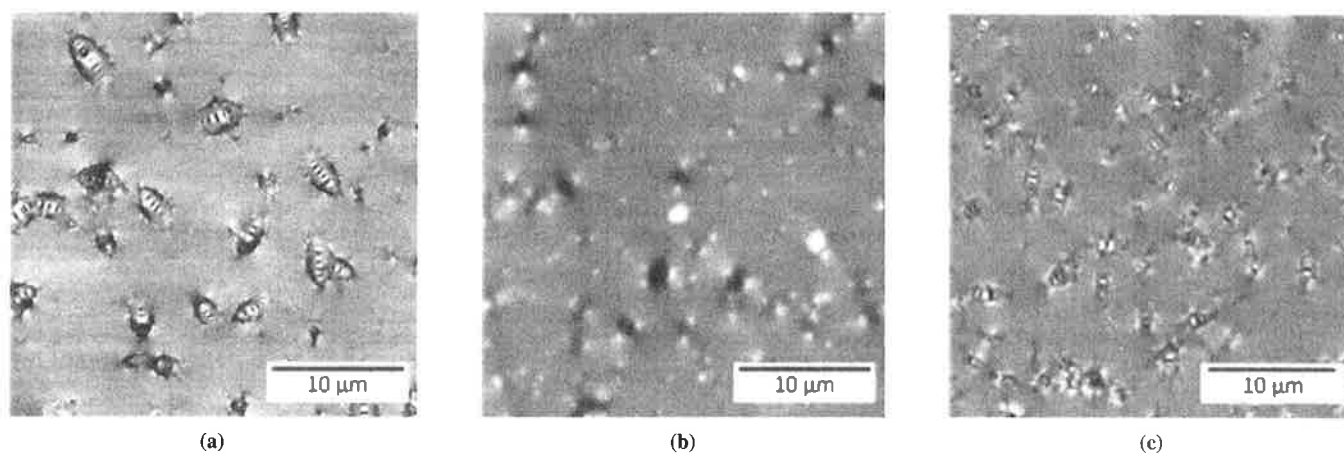


FIGURE 4 AFM images of (a) virgin asphalt binder, (b) extracted maltene phase, and (c) precipitated blend.

toluene, asphaltenes were redispersed in the maltene phase, and thus precipitated blends were produced.

To investigate whether the precipitated blends produced a microstructure similar to the virgin binder, AFM was carried out on the virgin binder, the pure maltene phase, and the precipitated blend with a comparable asphaltene concentration (7.77 vol%) (24). Topographical images of all three samples are shown in Figure 4. Figure 4a shows the virgin samples. The characteristic bee structure or cantana phase is clearly visible. Figure 4b shows the extracted maltene phase with no asphaltenes present in the sample. No cantana phase can be seen, whereas Figure 4c shows the bee structure reestablished in the precipitated blend. The AFM images in Figure 4 provide strong evidence that the procedure to create precipitated blends resulted in a microstructure similar to that of the virgin binder sample. Because the cantana phase was not visible in the pure maltene phase, it also could be taken as evidence that the inclusions were related to the presence of asphaltenes in the material.

CR tests were carried out on a dynamic shear rheometer to obtain the material behavior. Although a constant torque  $M$  was applied for 1,800 s on an asphalt binder film (diameter  $d = 25$  mm, height  $h = 1$  mm), the deflection  $\phi(t)$  was measured. From  $\tau = 2M/\pi \cdot r^3$  and  $\gamma = r \cdot \phi(t)/\pi$ , the creep compliance was obtained as

$$J_{\text{exp}}(t) = \frac{\gamma(t)}{\tau} \quad (1)$$

where

- $J$  = creep compliance (1/MPa),
- $t$  = time (s),
- $\gamma$  = shear strain (–), and
- $\tau$  = shear stress (MPa).

These tests were run at temperatures in a range from  $-5^{\circ}\text{C}$  to  $+15^{\circ}\text{C}$ . The full experimental program is given in Table 1.

Figure 5 shows the results of CR tests on unaged and lab-aged precipitated blends with varying asphaltene concentration at  $+5^{\circ}\text{C}$ . Three replicates were run for each material. Although an increase in asphaltene concentration caused a decrease in creep compliance and thus stiffer material behavior, the creep rate  $dJ/dt$  decreased with an increase in asphaltene concentration until almost elastic behavior was reached at an asphaltene concentration of 17.36 vol%.

The addition of only low amounts of asphaltenes (4.18 vol%) to the maltene phase led to a strong increase in stiffness (Figure 5, blue and green lines). The creep compliance at 1,800 s was at a mean value of 90 1/MPa for the pure maltene phase and dropped to a mean value of 20 1/MPa for the blend with 4.18 vol% of asphaltenes, which indicated an increase in stiffness by a factor of 4.5. This result showed that, through the addition of asphaltenes, a structure in asphalt binder was introduced that strongly affected the mechanical behavior, similar to what occurred when precipitation hardening was used in metal hardening. Another key finding was that aged and unaged samples with the same asphaltene concentrations showed no significant differences in their creep curves. This finding in turn meant that the material behavior of maltenes and asphaltenes was not affected by aging. Thus the detected increase in the asphaltene concentration from 7.79 vol% (unaged) to 13.36 vol% (RTFOT + PAV aged) mentioned in other studies (15, 17, 25) appeared to be the only, or at least the most important, consequence of aging on the microstructure of asphalt binder.

On the basis of the physicochemical and microscopic analysis of the binder, a concept of the microstructure of asphalt binder was proposed, which consisted of a continuous matrix of maltenes with asphaltene inclusions (Figure 6a). A structural concept of the representative volume element for micromechanical modeling is shown in Figure 6b. A representative volume element of asphalt binder has a continuous

TABLE 1 Test Program for CR Tests on Precipitated Blends

Asphaltene Concentration	Test Temperature		
	$-5^{\circ}\text{C}$	$+5^{\circ}\text{C}$	$+15^{\circ}\text{C}$
0 vol%	●/○	●/○	●/○
4.18 vol%	●/○	●/○	●/○
7.77 vol%	○	●/○	○
12.32 vol%	NA	●	●
17.36 vol%	○	●/○	○
26.71 vol%	NA	●	NA

NOTE: ○ = unaged sample; ● = RTFOT + PAV aged sample; NA = not available.

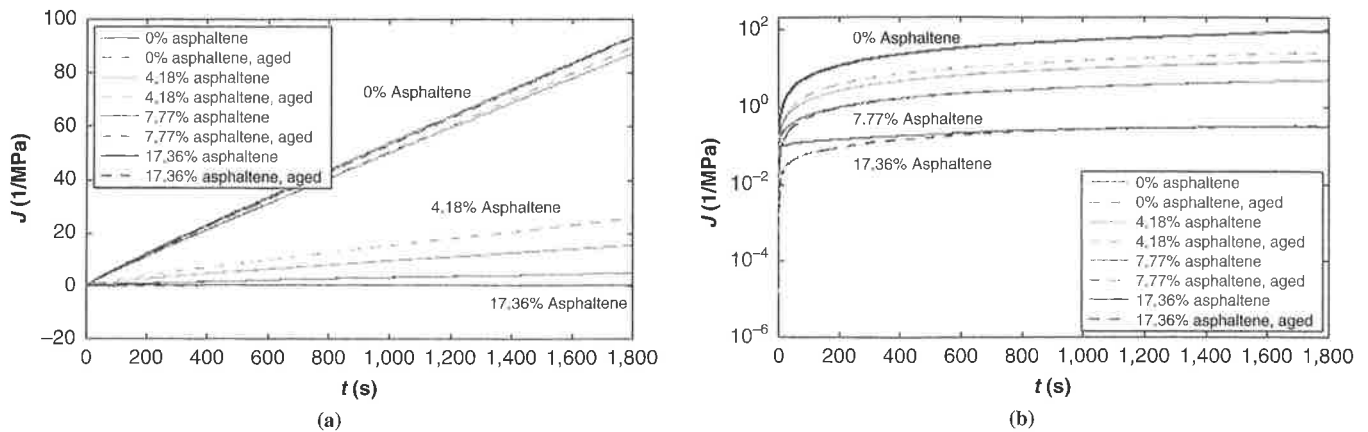


FIGURE 5 Results from CR tests on unaged and RTFOT + PAV-aged precipitated blends at +5°C: (a) linear and (b) logarithmic scale.

matrix of maltenes with spherical asphaltene inclusions. The network-like structure of shells around the asphaltenes is represented by an interaction phase, which appears as needles with arbitrary orientation.

With the micromechanical model (Figure 6b), the viscoelastic behavior of the asphalt binder can be predicted, given the aging-induced change of the material response as a result of increasing asphaltene concentration. For this reason, the identification of the model input parameters is a crucial task. The material properties of the maltene phase can be characterized directly by CR tests. The material behavior of asphaltenes, however, can be assessed indirectly through the backcalculation from CR test results of precipitated blends. Likewise, the volume fraction of the interaction phase can be obtained. As outlined in Aigner et al., the power law model used to describe the mechanical behavior of asphalt binder and its constituents describes the experimentally obtained viscoelastic response well (26). The consequent implication is a physically relevant form of Equation 2 according to Füssl et al. (27), which reads as follows:

$$J_{\text{mod}}(t) = J_0 + J_a \left( \frac{t}{\tau} \right)^k \quad (2)$$

where

$J_0$  = creep compliance of the spring in the power law model (1/MPa),

$J_a$  = creep compliance of the fractional dashpot in the power law model (1/MPa), and

$k$  = behavior of the fractional dashpot (-).

To identify the parameters  $J_{0,\text{malt}}$ ,  $J_{a,\text{malt}}$ , and  $k_{\text{malt}}$  of the maltene phase, the error between experimentally obtained creep compliances  $J_{\text{exp}}$  from CR identification tests and predicted creep compliances  $J_{\text{mod}}$  was minimized through nonlinear least square fitting. The obtained power law parameters for the maltene phase at -5°C, +5°C, and +15°C described almost perfect fits (Table 2).

As discussed, power law parameters of asphaltenes and the interaction phase were backcalculated from the experimental results of precipitated blends with an asphaltene concentration of 4.18 vol% at a temperature of +5°C with the coefficient of determination  $R^2$  as an indicator for the degree of accordance. It was thereby determined that the parameters  $J_{0,\text{aspha}}$ ,  $J_{a,\text{aspha}}$ , and  $k_{\text{aspha}}$ , which were applicable to asphaltenes as well as to the interaction phase, lay within a range in which their influence on the predicted material response could be considered insignificant (28).

Because the needle-shaped interaction phase described the structural influence of the asphaltene micelle network, its volume fraction  $f_{ip}$  was directly related to the asphaltene concentration. Similar to the power law parameters, the volume fraction of the interaction phase  $f_{ip}$  was determined on a best-fit basis and employed  $R^2$  to evaluate the degree of accordance. When asphaltene and backcalculated needle content were correlated, an exponential relation was found for (realistic) asphaltene concentrations up to 17.36 vol% (Figure 7). This result was typical (e.g., for molecular agglomeration processes in nature).

With all of the input parameters available, model predictions were compared with experimental results from aged precipitated blends with asphaltene concentrations of 4.18 vol%, 7.77 vol%, 12.32 vol%, and 17.36 vol% (Figure 8). Besides the known volume fraction of

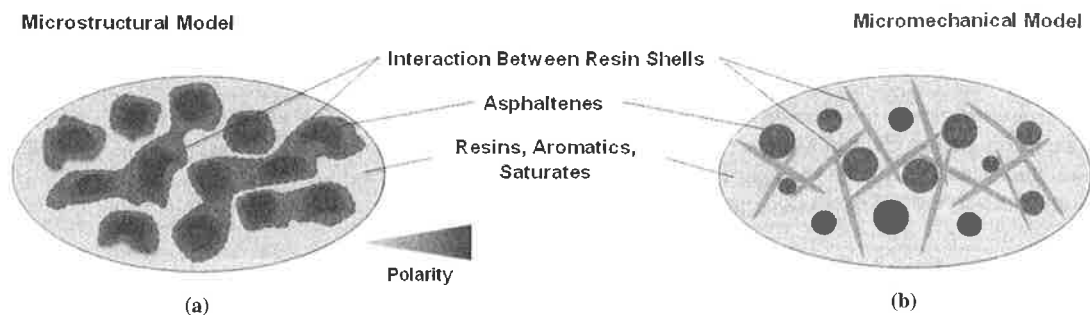


FIGURE 6 Proposed concept of (a) microstructural model and (b) micromechanical representation.

**TABLE 2 Power Law Parameters for Maltene Phase**

Power Law Parameter	Test Temperature		
	-5°C	+5°C	+15°C
$J_{0,malt}$ [1/MPa]	0.0980	0.2652	2.433
$J_{a,malt}$ [1/MPa]	0.0076	0.0766	1.205
$k_{malt}$ [-]	0.8124	0.9386	1.027
$R^2$	.99	.99	.99

the asphaltenes, the content of the interaction phase was the only parameter that varied.

To validate the proposed model, CR tests were run not only on precipitated blends but also on original asphalt binders, including unaged STA (RTFOT) and LTA (RTFOT + PAV) unmodified PG 58-22 samples with known asphaltene concentrations. The results can be seen in Figure 9.

The experimental results were related to model predictions, which took the actual asphaltene concentrations into account. As can be seen

in Figure 9, the prediction of LTA (i.e., asphaltene concentration of 13.36 vol%) fit the experimental results well. As described earlier, the binder samples had to be heated to identify the asphaltene concentration through n-heptane extraction. Because the asphaltene concentration (n-heptane nonsoluble phase) is strongly affected by heating as a result of aging, its determination is a challenging task. A reliable specification of the amount of asphaltenes is difficult, especially for unaged and short-term aged samples, which are more susceptible to aging effects than samples already aged over the long term. However, model predictions that considered a realistic asphaltene concentration for unaged and short-term aged samples to be between 4 vol% and 9 vol% correlated well with the experimental results.

**SUMMARY AND CONCLUSIONS**

A microphysical and micromechanical model on binder aging was developed through interdisciplinary research into the fundamentals of asphalt binder aging on the physicochemical and mechanical level. The following conclusions could be drawn:

- LTA (oxidative) of asphalt binder in the field may be triggered not only by atmospheric oxygen but also by other reactive gases

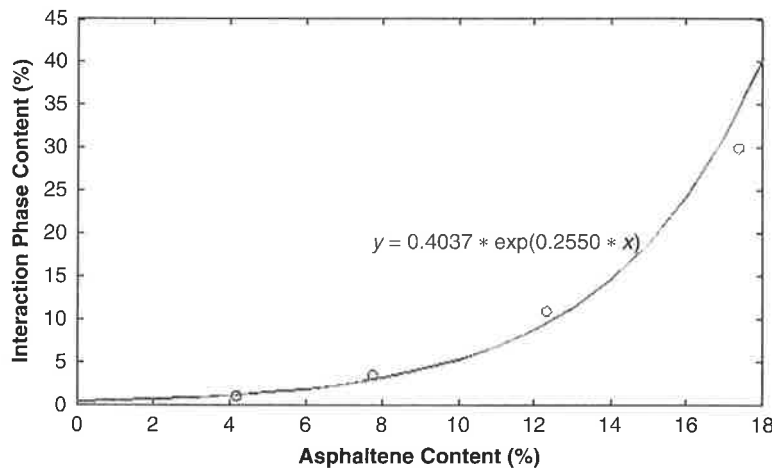


**FIGURE 7** Exponential relation between asphaltene and needle content (interaction between micelle mantles).

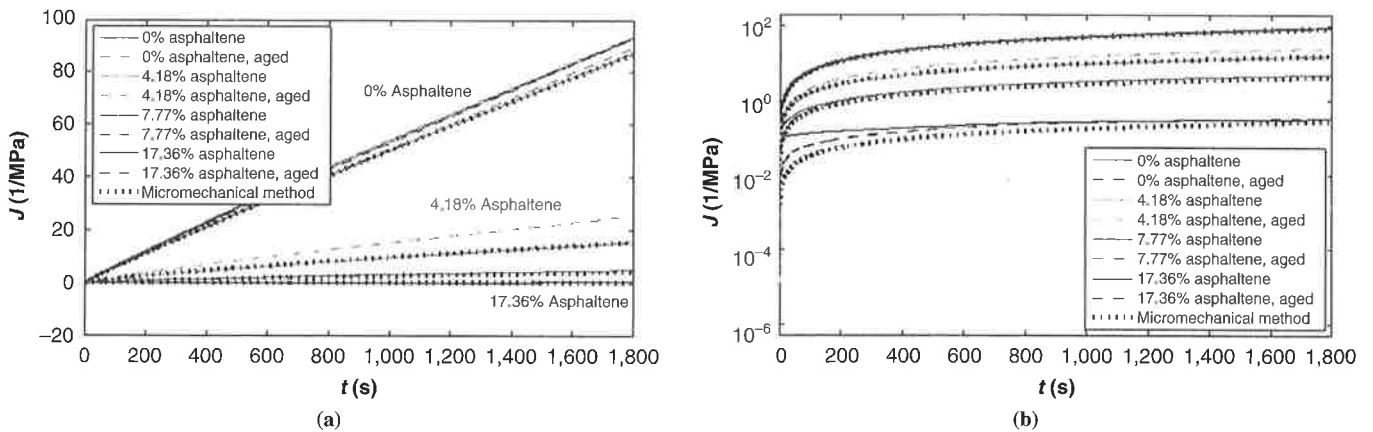


**FIGURE 8** Comparison of experimental results and micromechanical model predictions for precipitated blends at +5°C: (a) linear and (b) logarithmic scale.

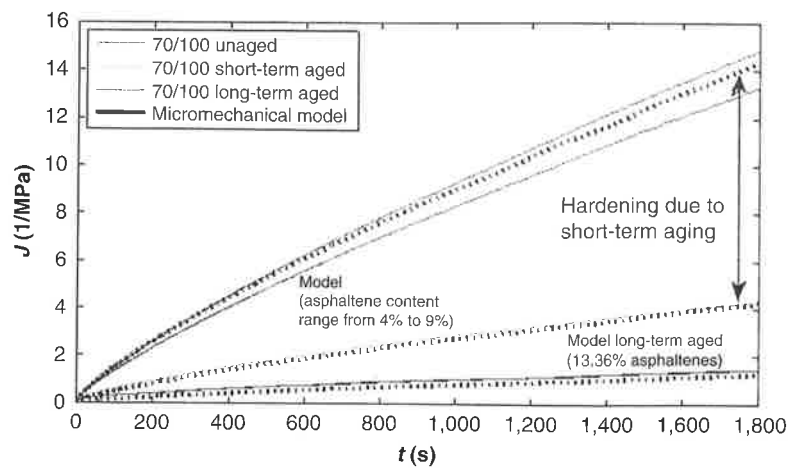


FIGURE 9 Comparison of experimental results and micromechanical model predictions for unaged, RTFOT-aged, and RTFOT + PAV-aged asphalt binder PG 58-22.

(e.g., nitric oxides, ozone). These gases are available in much smaller concentrations but have a significantly higher oxidation potential than atmospheric oxygen at temperatures that occur in the field ( $< +65^{\circ}\text{C}/150^{\circ}\text{F}$ ). Water soluble oxidants (e.g.,  $\text{HNO}_3$ ,  $\text{H}_2\text{SO}_4$ ,  $\text{H}_2\text{O}_2$ ) can penetrate into binder and base layers and promote aging in these layers.

- A microphysical model on asphalt binder aging on the basis of the idea of the micelle model explains LTA by oxidation through changes in the polarity distribution within matrix, mantle, and micelle. An increasing gap in polarity as a result of oxidation may explain the macroscopic effect of increasing brittleness associated with binder aging.

- It was shown by AFM that precipitated blends produced from fractionated maltenes and asphaltenes exhibited a microstructure similar to that of the original asphalt binder. The presence of asphaltenes seemed to be responsible for the formation of the bee structure or cantana phase.

- Mechanical analysis of precipitated blends with different concentrations of asphaltenes showed that, through the addition of asphaltenes to the maltene phase, a networklike structure in the asphalt binder was introduced. This addition strongly affected the mechanical behavior in terms of increasing stiffness.

- Comparative mechanical analysis of precipitated blends from unaged and long-term aged (RTFOT + PAV) samples indicated that an increase in asphaltene concentration with aging was the only consequence of aging, or at least the most important one, for mechanical behavior in terms of increasing stiffness.

- A micromechanical model was established to explain the macroscopic, mechanical binder behavior on the basis of the behavior of the maltene phase and the asphaltenes. The mechanical behavior of unaged, short-term and long-term aged asphalt binders could be predicted through employment of the model.

## ACKNOWLEDGMENTS

The authors thank the Austrian national research promotion agency and the industrial partners of the Oekophalt project for cofinancing the research.

## REFERENCES

1. Huang, S.C., A.T. Pauli, R.W. Grimes, and F. Turner. Ageing Characteristics of RAP Binder Blends: What Types of RAP Binders Are Suitable for Multiple Recycling? *Road Materials and Pavement Design*, Vol. 15, Suppl. 1, 2014, pp. 113–145.
2. Ongel, A., and M. Hugener. Aging of Bituminous Mixes for Rap Simulation. *Construction and Building Materials*, Vol. 68, 2014, pp. 49–54.
3. Liu, G., E. Nielsen, J. Komacka, L. Greet, and M. van de Ven. Rheological and Chemical Evaluation on the Ageing Properties of SBS Polymer Modified Bitumen: From the Laboratory to the Field. *Construction and Building Materials*, Vol. 51, 2014, pp. 244–248.
4. da Costa, M.S., F. Farcas, L. Santos, M.I. Eusebio, and A.C. Diogo. Chemical and Thermal Characterization of Road Bitumen Ageing. In *Advanced Materials Forum V, Parts 1 and 2* (L.G. Rosa and F. Margarido, eds.), Trans Tech Publications Ltd., Stafa-Zurich, Switzerland, 2010, pp. 273–279.
5. Hagos, E.T., A.A.A. Molenaar, and M.F.C. van de Ven. Chemical Characterization of Laboratory and Field Bitumen Aging in Porous Asphalt Concrete. *Advanced Testing and Characterisation of Bituminous Materials*, Vol. 1–2, 2009, pp. 173–184.
6. Le Guern, M., E. Chailleux, F. Farcas, S. Dreessen, and I. Mabile. Physicochemical Analysis of Five Hard Bitumens: Identification of Chemical Species and Molecular Organization Before and After Artificial Aging. *Fuel*, Vol. 89, No. 11, 2010, pp. 3330–3339.
7. Poulidakos, L.D., S. dos Santos, M. Bueno, S. Kuentzel, M. Hugener, and M.N. Partl. Influence of Short and Long Term Aging on Chemical, Microstructural, and Macro-Mechanical Properties of Recycled Asphalt Mixtures. *Construction and Building Materials*, Vol. 51, 2014, pp. 414–423.
8. Allen, R.G., D.N. Little, A. Bhasin, and C.J. Glover. The Effects of Chemical Composition on Asphalt Microstructure and Their Association to Pavement Performance. *International Journal of Pavement Engineering*, Vol. 15, No. 1, 2014, pp. 9–22.
9. Fernandez-Gomez, W.D., H.R. Quintana, and F.R. Lizcano. Review of Asphalt and Asphalt Mixture Aging. *Ingenieria E Investigacion*, Vol. 33, No. 1, 2013, pp. 5–12.
10. Zhang, H.L., J.Y. Yu, Z.G. Feng, L.H. Xue, and S.P. Wu. Effect of Aging on the Morphology of Bitumen by Atomic Force Microscopy. *Journal of Microscopy*, Vol. 246, No. 1, 2012, pp. 11–19.
11. Hofko, B., R. Blab, L. Eberhardsteiner, J. Fuessler, H. Grothe, F. Handle, and M. Hospodka. Impact of Field Ageing of Binder on Performance of Hot Mix Asphalt. *Proc., 12th ISAP Conference on Asphalt Pavements*, Raleigh, N.C., 2014.
12. Petersen, J.C., T. Robertson, J.F. Branthaver, P.M. Harnsberger, J.J. Duvall, S.S. Kim, D.A. Anderson, D.W. Christiansen, H.U. Bahia, R. Dongré, M.G. Sharma, J.W. Button, and C.J. Glover. *SHRP-A-370*:

- Binder Characterization and Evaluation Volume 4: Test Method*. National Research Council, Washington, D.C., 1994.
13. Handle, F. Bitumen Structure and Bitumen Ageing. *Proc., 15th Austrian Chemistry Days*. Graz, Austria, 2013.
  14. von Reinhard Zellner, H. Chemie über den Wolken: . . . und darunter. *Angewandte Chemie*, Vol. 123, No. 43, 2011, pp. 10196–10197.
  15. Lesueur, D. The Colloidal Structure of Bitumen: Consequences on the Rheology and on the Mechanisms of Bitumen Modification. *Advances in Colloid and Interface Science*, Vol. 145, No. 1–2, 2009, pp. 42–82.
  16. Redelius, P. Asphaltenes in Bitumen: What They Are and What They Are Not. *Road Materials and Pavement Design*, Vol. 12, No. 4, 2011, pp. 795–819.
  17. Read, J., and D. Whiteoak. *Shell Bitumen Handbook*, 5th ed. Thomas Telford Ltd., London, 2003.
  18. Solaimany-Nazar, A. R., and H. Rahimi. Investigation on Agglomeration–Fragmentation Processes in Colloidal Asphaltene Suspensions. *Energy and Fuels*, Vol. 23, No. 2, 2009, pp. 967–974.
  19. Sheu, E. Y. Physics of Asphaltene Micelles and Microemulsions: Theory and Experiment. *Journal of Physics: Condensed Matter*, Vol. 8, No. 25A, 1996, pp. A125–A141.
  20. Fawcett, A., and T. McNally. Polystyrene and Asphaltene Micelles Within Blends with a Bitumen of an SBS Block Copolymer and Styrene and Butadiene Homopolymers. *Colloid and Polymer Science*, Vol. 281, No. 3, 2003, pp. 203–213.
  21. Eyssautier, J., I. Hénaut, P. Levitz, D. Espinat, and L. Barré. Organization of Asphaltenes in a Vacuum Residue: A Small-Angle X-ray Scattering: Viscosity Approach at High Temperatures. *Energy and Fuels*, Vol. 26, No. 5, 2012, pp. 2696–2704.
  22. Pollack, S. S., and T. F. Yen. Structural Studies of Asphaltics by X-Ray Small Angle Scattering. *Analytical Chemistry*, Vol. 42, No. 6, 1970, pp. 623–629.
  23. Tripadus, V., M. Popovici, M. Peticila, L. Craciun, and O. Muresan. Study of Diffusive Motion in Bitumen Compounds by Quasielastic Neutron Scattering. *Physica B: Condensed Matter*, Vol. 350, No. 1–3, 2004, pp. E455–E458.
  24. Hofko, B., R. Blab, L. Eberhardsteiner, J. Füssl, H. Grothe, F. Handle, M. Hospodka, S. Nahar, A. Schmets, and A. Scarpas. Microstructure and Rheology of Bitumen: Friends or Foes? *Materials and Structures*, 2014.
  25. Grover, R. A. *Structural Characterization of Micromechanical Properties in Asphalt Using Atomic Force Microscopy*. MS thesis. Texas A&M University, College Station, 2010.
  26. Aigner, E., R. Lackner, and C. Pichler. Multiscale Prediction of Viscoelastic Properties of Asphalt Concrete. *Journal of Materials in Civil Engineering*, Vol. 21, No. 12, 2009, pp. 771–780.
  27. Füssl, J., R. Lackner, and J. Eberhardsteiner. Creep Response of Bituminous Mixtures: Rheological Model and Microstructural Interpretation. *Meccanica*, Vol. 49, No. 11, 2013.
  28. Eberhardsteiner, L., J. Füssl, B. Hofko, R. Blab, H. Grothe, F. Handle, and M. Hospodka. Influence of Asphaltene Content on Bitumen Behavior: Experimental Investigation and Micromechanical Modeling. *Materials and Structures*, 2014. <http://link.springer.com/article/10.1617%2Fs11527-014-0383-7>.
- 
- The Standing Committee on Characteristics of Asphalt Materials peer-reviewed this paper.*